National Bureau of Standards

February 1958
Volume 42
Number 2

Technical News Bulletin

Technology

Redetermination of the Standard Ampere

A RECENT EXPERIMENT at the National Bureau of Standards has shown that the standard ampere maintained by the Bureau has drifted no more than a few parts per million in the last 15 years.[1] Such a small apparent change may well be due to slight errors in measurement so that the standard ampere may actually have remained almost perfectly stable since its original evaluation in 1942.

Because of the importance of precise electrical measurements to modern science and industry, the Bureau maintains permanent primary standards of two basic electrical quantities, voltage and resistance.[2] From these basic electrical standards, the Bureau has derived other standards for all electrical quantities in use today. One of these, of course, is electric current. Because current is transitory, the primary standard ampere cannot be kept in the form of a material object such as the standard cells that maintain the volt or the standard resistors that maintain the ohm. Each time the standard ampere is required, it must be obtained anew from the standard volt and the standard ohm by use of Ohm's law. However, a gradual change might sometimes occur in the standard cells or the standard resistors. One method of checking the stability of these standards is to compare the standard ampere derived from them with the "absolute" ampere, that is, the ampere obtained experimentally in terms of mechanical units of length, mass, and time.

In the present determination, R. L. Driscoll and R. D. Cutkosky of the Bureau staff measured the standard ampere in absolute amperes using two different sets of apparatus. One was the current balance used in the 1942 evaluation; [3] the other was a Pellat type electrodynamometer, which was introduced to reduce the possibility of systematic errors. The standard ampere was found to equal 1.000008 absolute amperes by the current balance method and 1.000013 absolute amperes by the Pellat instrument. The weighted mean of these two values is 1.000010 absolute amperes, but in this mean there is an uncertainty of 5 parts per million. If no accidental errors were made in either the original or the present evaluation, and if all systematic errors remained fixed, then the value of the current yielded by the electrical standards of resistance and voltage has decreased by 6 parts per million. On the other hand, known sources of accidental error in the current balance determinations could easily account for the apparent drift.

Current Balance

The ampere was evaluated with helical coils by determining the mechanical force between the two parts of the circuit through which the current flows. In the center of two large fixed coils, a smaller coil is hung from the arm of a precision balance. All three coils carry the current to be measured, but the current in the fixed coils can be reversed. The electromagnetic force developed by the current in the coils tends to pull the movable coil downward for one direction of the current

452553—58

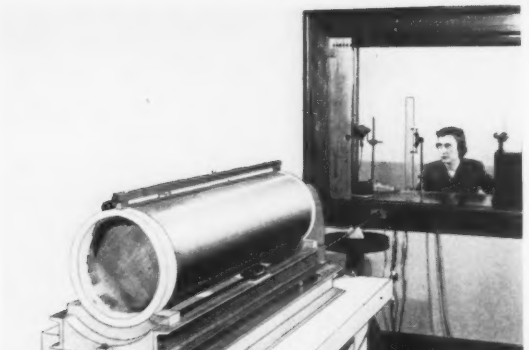

Determining the absolute value of the ampere with a Pellat balance. The equipment is operated from another room to avoid air disturbance and dimensional changes produced by heat from the body.

in the fixed coils but tends to lift it when this current is reversed. From the change in the force on the balance when the current is reversed and from the measured dimensions of the coils, the value of the current in absolute amperes can be computed. The uncertainty in this method arising from all known sources is estimated to be 6 parts per million.

Electrodynamometer

The modified Pellat electrodynamometer consists essentially of a long stationary horizontal solenoid 28 cm in diameter, a short solenoid 11.6 cm in diameter, and a balance. The smaller coil, which is mounted on the balance beam, is inserted into the longer solenoid so that the coil axes are perpendicular. Current in the outer solenoid produces a magnetic field which is essentially constant at its center. When the coils are connected in series, an electromagnetic torque on the smaller solenoid is produced. The small coil therefore tends to tip. Since the balance beam rests on a knife edge, the tipping of the coil attached to the beam upsets the balance. The system is restored to equilibrium with a suitable counterweight. When the current in the stationary coil is reversed, the coil tips the other way and equilibrium is restored by placing a mass on the end of the balance arm.

During this operation, the current was held constant at about 1.02 amperes, the value being determined by the standard cell and standard resistor. These standards were maintained at constant temperature and compared from time to time with the Bureau's primary standards. The mass that counteracted the change in torque was adjusted by trial and later evaluated by comparison with known standards. A calibrated scale on the balance allowed for small corrections to the balancing mass. From the known value of the balance weight, the length of the balance arm, and the geometry of the windings, the value of the current was calculated.

The Bureau's electrodynamometer differs from Pellat's original in several ways. One such difference is its single-layer helical windings. The dimensions of the single-layer windings can be easily checked, whereas the uncertainty in the dimensions of the original balance windings introduced error. The materials used in constructing the coils also differ from those used in the original. The stationary coil form and balance beam are of fused silica, the rotatable coil form is Pyrex glass, and the winding is of oxygen-free copper wire. Special care was taken to insure low magnetic susceptibility in all parts. For example, aluminum alloys were used in the balance supports, and the brass and phosphor bronze parts of the balance-arrestment mechanism were tested for susceptibility.

The pitch of the stationary coil, the diameter of the rotatable coil and the length of the balance arm are critical parameters in the current evaluation. In making an accurate determination, the pitch of the stationary coil was measured by a micrometer method. Longitudinal readings for the measurement of pitch were taken at

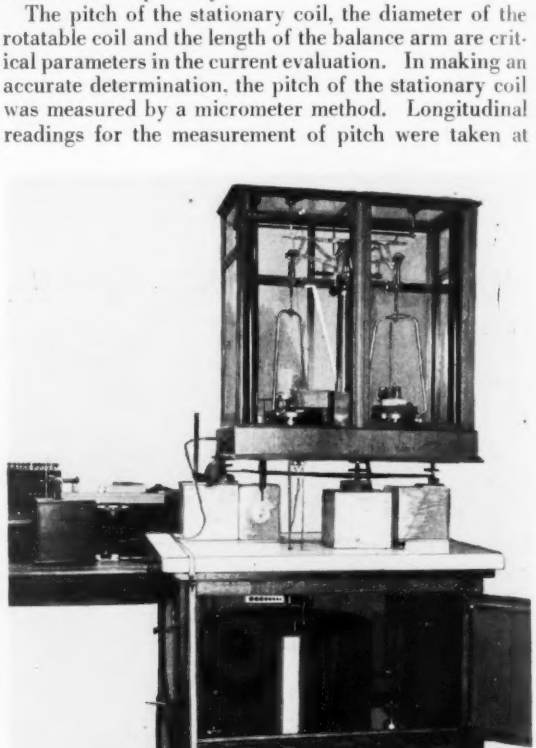

Over-all view of the helical coil balance. In the center of the coil (bottom) is a small movable coil which is attached to the arm of the precision balance. This arrangement measures the change in force on the small current-carrying coil when current in the two parts of the outer coil is reversed. From the change in force and the dimensions of the coils, the value of the current in amperes is obtained.

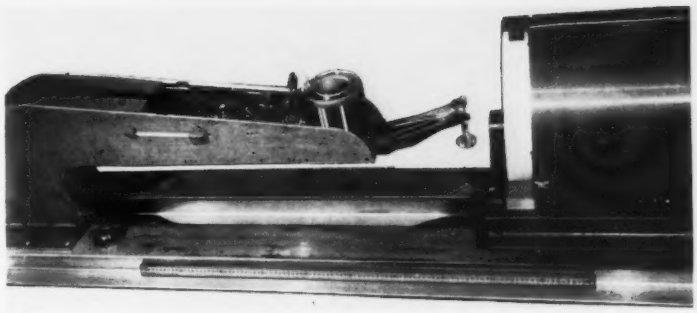

Electrodynamometer used in the re-evaluation of the standard ampere. When the smaller rotatable coil is inserted into the larger stationary coil, the current flowing through the coils produces a torque. The small coil is connected to a balance so that as it tips, equilibrium is upset. Balance is restored by adding known weights to the balance arm. From the known weight, the length of the balance arm, and the geometry of the windings, the value of the current can be calculated.

several places along the coil in each of six angular positions around the winding. The diameters of both coils were also measured with considerable precision. Although the stationary coil diameter did not have to be known accurately for the current evaluation, such a measurement is necessary should the coil be developed into a standard of inductance. The uncertainty in this method is 8 parts per million. The major source of this uncertainty is the limited accuracy with which the radius of the rotatable coil could be measured. The Bureau considers it possible to ultimately reduce uncertainty in the radius measurement by a factor of two so that the electrodynamometer will be as accurate an instrument as the current balance.

---

[1] Measurement of current with the NBS current balance, *by R. L. Driscoll and R. D. Cutkosky, J. Research NBS (in press)*; Measurement of current with a Pellat type electrodynamometer, *by R. L. Driscoll, J. Research NBS (in press)*.

[2] Standards for electrical measurement, *NBS Tech. News Bul.* **34**, *176 (December 1950)*.

[3] An absolute determination of the ampere, using helical and spiral coils, *R. W. Curtis, R. L. Driscoll, and C. L. Critchfield, J. Research NBS* **28**, *133 (1942) RP1449*.

Impact Behavior of Plastics

TO be able to predict how plastic materials react to high-speed impact is of increasing significance to industry and to national defense. Among products fabricated of plastics which must withstand high-speed impact are the safety helmets and goggles worn by workers in hazardous occupations; the body armor used by the armed services; and the disposable parachutes employed to deliver emergency supplies by air. As part of a broad program to develop data on the properties of materials, the Bureau recently undertook an investigation [1] of the impact behavior of typical plastics. The work was sponsored by the Office of the Quartermaster General, Department of the Army.

An impacting machine, previously developed to study the stress-strain relationship in yarns,[2] was adapted to test plastic film by Charles F. Bersch, Frank L. McCrackin, and Karl F. Plitt of the staff. A motion-picture camera, operating at about 7,000 frames per second, automatically recorded the effect of the impact. Data derived from such a photographic record are expected to be of value in developing more effective energy-absorbing plastics; in studying the relation of molecular structure and physical behavior; and in developing theories for predicting the behavior of materials similar to plastics.

The impacting machine consists principally of a flywheel, fitted with a pair of hammers and driven by a 5-hp variable-speed motor. In performing the tests, a strip of plastic film about 65-cm long and 3-mm wide is used. Head and tail masses are attached to the two ends of the specimen which is inserted, fully extended, in a clear plastic tube and mounted on the machine. While the wheel is being accelerated, the hammers pass on either side of the rectangularly-shaped head mass protruding from one end of the plastic tube. When the desired velocity is reached, the tube is rotated 90° so that the head mass is impacted by the hammers at a speed of from 40 to 80 meters a second.

Strip of plastic film, with head and tail masses attached. This specimen is 3-mm wide and 65-cm long.

After impact, the specimen and head and tail masses move in free flight. This motion is photographed against a background containing a centimeter scale, with mirrors arranged to reflect images of both the head

Consecutive frames from the motion-picture film arranged horizontally showing head mass in flight immediately after impact. Slight movement of the tail mass may be noted in the upper half of the frames.

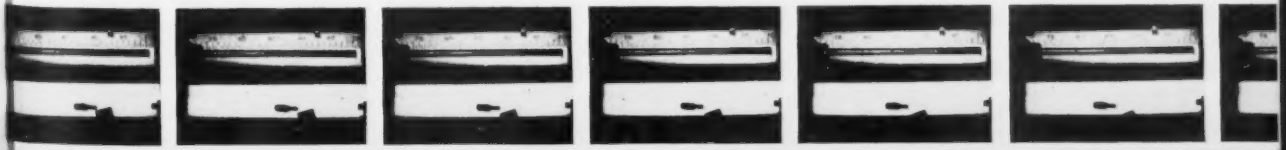

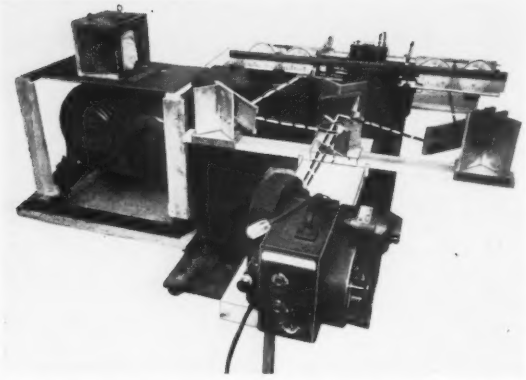

Equipment used to perform high-speed impact tests on plastic film. The variable-speed motor is on the left with catch box mounted above; high-speed camera is in the foreground; tube containing specimen is mounted in front of the scale in the background. Broken lines indicate path of light beams from the head and tail masses as reflected in the mirror system in the center.

and tail masses on each frame of the film. After the test, the positions of the head and tail masses are measured for each frame. Rates of straining of from 400,000 to 800,000 percent per minute are obtained.

The theoretical analysis of this high-velocity impact method previously presented in detail by McCrackin et al.[3] and by Smith et al.[4 5] was modified to get an expression for the energy necessary to rupture a specimen under the conditions of the study. For polyester film, the energy to rupture, the strain at rupture, and the residual strain were found to be about 25 percent less at rates of straining of from 400,000 to 800,000 percent per minute than at rates of straining of from 1- to 100-percent per minute. The latter rates of straining are used for normal testing.

Specimens were cut parallel to both the length and width of the sheet of film used. No significant changes were found, at either high or low rates of straining, between the rupture energies measured on both types of specimens. The recovered strain, which is an approximation of the elasticity of the material, was relatively constant for all rates of straining.

---

[1] *For further technical details, see* Effects of rates of straining on some tensile properties of polyester film, *by C. F. Bersch, F. L. McCrackin, and K. F. Plitt, Modern Plastics* **35,** *171 (1957).*

[2] Stress-strain relationships in yarns subjected to rapid impact loading: 1. Equipment, testing procedure, and typical results, *by W. K. Stone, H. F. Schiefer, and G. Fox, J. Research NBS* **54,** *269 (1955) RP2589;* Shock loading of textile yarns, *NBS Tech. News Bul.* **40,** *91 (1956).*

[3] Stress-strain relationships in yarns subjected to rapid impact loading: 2. Breaking velocities, strain energies, and theory neglecting wave propagation, *by F. L. McCrackin, H. F. Schiefer, J. C. Smith, and W. K. Stone, J. Research NBS* **54,** *277 (1955) RP2590; also in Textile Research Journal* **25,** *529 (1955).*

[4] Stress-strain relationships in yarns subjected to rapid impact loading: 3. Effect of wave propagation, *by J. C. Smith, F. L. McCrackin, and H. F. Schiefer, J. Research NBS* **55,** *19 (1955) RP2601; also in Textile Research Journal* **25,** *701 (1955).*

[5] The impact-absorbing capacity of textile yarns, *by J. C. Smith, F. L. McCrackin, and H. F. Schiefer, ASTM Bul. No. 220, 52 (1957).*

X-Ray Penetration in Lead

THE ENERGY and angular distribution of photons emerging from a lead barrier exposed to 8- and 10-million electron volt X-rays have been determined by the Bureau.[1] The experiment was undertaken by J. H. Hubbell, E. Hayward, and W. F. Titus to obtain previously undetermined data on transmitted radiation at high energies. Their results not only provide design data for nuclear equipment shielding but also verify the mathematical and computational methods now used in solving penetration problems.

Below 1 Mev, some discrepancies were found between the computational and experimental results. As the mathematical theory was designed for an infinite medium, these variations may be due to the presence of a boundary in the experiment. Since good correspondence has been obtained at higher energies, the present study may prove useful in modifying the infinite medium theory to take into account the presence of a boundary.

This experiment was the third of a series[2] undertaken by the Bureau to check the results of calculations based on the moments theory[3] of Bureau scientists L. V. Spencer and U. Fano. These calculations take into account multiple Compton collisions but treat photoelectric effect and pair production as absorption phenomena. Secondary radiations such as bremsstrahlung, fluorescence, and annihilation radiation are neglected. Experimental results obtained with the first two experiments using Co^{60} radiation at approximately 1 Mev agreed satisfactorily with calculated values. However, data at higher energies were required for a complete comparison.

The 8- and 10-Mev X-rays were bremsstrahlung beams produced in a 50-Mev betatron.[4] The betatron beam, collimated to produce a beam 9 in. in diameter, was used to irradiate a stack of lead sheets. Bremsstrahlung radiation incident on the plates was monitored by an ionization chamber.

Photons emitted by the lead barrier were detected by a scintillation spectrometer, consisting of a sodium-iodide (thallium-activated) crystal. The dissipation of energy in such a crystal produces a visible light pulse, which is detected and measured with the help of a photomultiplier tube. The photomultiplier converts the light output to an electrical pulse with a height proportional to the energy absorbed in the crystal detector. These pulses, transmitted by a cathode follower, were fed into the betatron control room, amplified, and analyzed by a 30-channel pulse-height analyzer.

The pulse-height distributions produced by the transmitted photons were measured at 0°, 5°, 10°, 20°, 30°, 40°, 50°, 60°, and 70° to the beam direction.

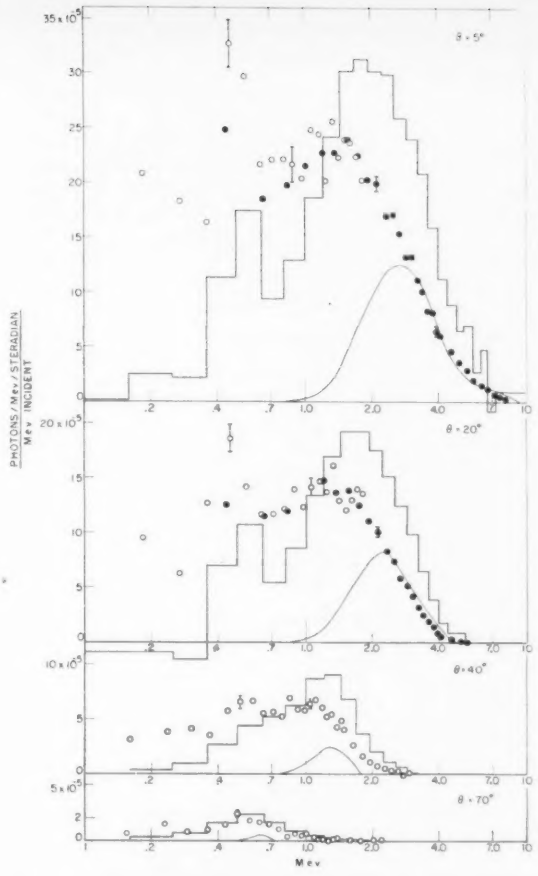

Energy distributions obtained at angles of 5°, 20°, 40°, and 70° by bombarding a 6-in. lead barrier with 10-Mev bremsstrahlung. The solid and open circles represent the experimental pulse-height data, and the histograms are obtained by multiplying the pulse-height data by an inverse detector-response matrix. The solid curves are the result of a calculation and represent the contribution to be expected from single scattering alone. The errors indicated are statistical.

These measurements were taken using a 6-in. lead barrier irradiated with both 8- and 10-Mev bremsstrahlung. Thicker barriers resulted in an attenuation which lowered the beam intensity beyond detection. It was not possible to extend the experiments to higher energies because the background—due to neutron capture gamma rays generated in the counter shielding—became too great.

In order to obtain the energy spectra of transmitted radiation, a matrix inversion of the experimentally-measured pulse-height data was employed. The spectra of transmitted energy show that photon energies and intensities change with angle and that multiple scattering predominates over single scattering.

In absolute magnitude and general shape, the theoretically-predicted and experimental penetration spectra agree. Except for energies below 300 Kev, the experimental numbers are slightly larger than the calculated ones. The secondary processes omitted from the calculation probably account for part of the discrepancy. The higher values in the measured distributions for photon energies above 1 Mev may be attributed to the bremsstrahlung by secondary electrons.

Below 1 Mev the presence of annihilation radiation masks the rest of the distribution. Subtraction of the calculated annihilation-radiation component reveals that fewer photons are detected than are predicted by the infinite medium calculations. The semi-infinite medium involved in the experiment undoubtedly influences the low-energy end of the spectrum. Since a photon must undergo a deflection larger than 90° to acquire low final energy, most of the low-energy photons travel backwards and thus escape detection.

---

[1] Energy and angular distribution of X-rays scattered in lead, *by J. H. Hubbell, E. Hayward, and W. F. Titus, Phys. Rev.* **108,** *1361 (1957).*

[2] The penetration and diffusion of Co^{60} gamma-rays in water using spherical geometry, *by G. R. White, Phys. Rev.* **80,** *154 (October 15, 1950);* The electron spectra produced by a Co^{60} source in water, *by E. Hayward, Phys. Rev.* **86,** *493 (May 15, 1952).*

[3] Penetration and diffusion of X-rays. Calculation of spatial distributions by polynomial expansion, *by L. V. Spencer and U. Fano, J. Research NBS* **46,** *446 (June 1951) RP2213;* Penetration and diffusion of gamma rays, *NBS Tech. News Bul.* **40,** *144 (October 1956).*

[4] Research in high-energy X-rays, *NBS Tech. News Bul.* **38,** *173 (December 1954).*

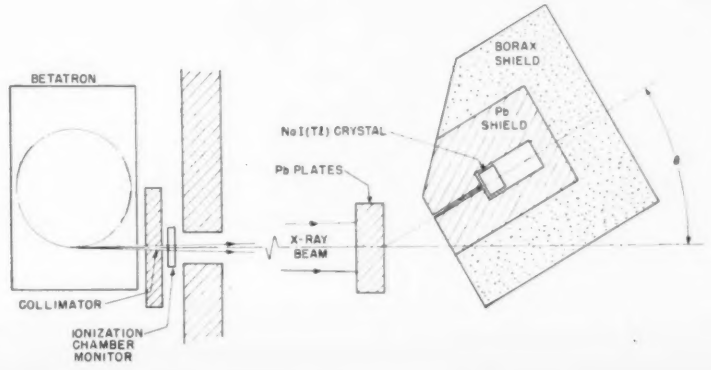

Experimental arrangement used to study the scattering of X-rays in lead. An X-ray beam from the betatron is collimated and used to irradiate a stack of lead plates. The betatron output is monitored by an ionization chamber, and the photons which penetrate the lead barrier are detected at various angles by a sodium-iodide (thallium-activated) crystal spectrometer shielded by lead and borax.

The Sag Point

a reference in heating glasses

TO COMPARE the thermal behavior of glasses of various compositions, some reference point must be defined. In comparing crystalline substances, melting temperatures are usually employed as references, but the melting of glass is a continuous process which occurs over a temperature range. However, other physical changes, such as softening and deformation, occur in the melting processes at definite temperatures. These have therefore been established as reference points. The Bureau has recently suggested the use of an additional reference, the "sag point".[1] This is the temperature at which a glass fiber of given dimensions, supported at established intervals, sags under its own weight. The sag point is highly reproducible and can be determined more rapidly and easily than the older reference points.

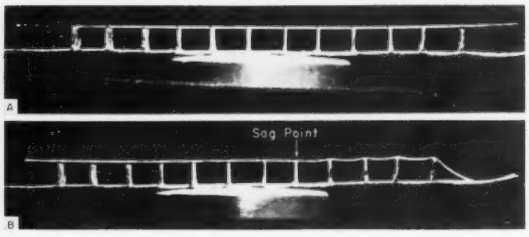

A, Glass fiber mounted on platinum specimen holder before heating. The supports are separated by ½-in. intervals. B, Fiber and holder after heating. Glass heated in the hotter region of the furnace has sagged. The temperature at which sagging first occurs is used as a reference point in annealing.

The need for such a reference arose in connection with research on new optical glasses at the Bureau. These experimental glasses had widely different compositions and consequently greatly varying physical properties. So that all the glasses could be annealed at the same stage of viscosity, a common reference point was required along with a simple rapid method for determining the temperature at which this point occurs in each glass. The use of the sag point was first suggested by C. A. Faich, formerly with the Bureau. S. Spinner, G. W. Cleek, and E. H. Hamilton of the mineral products laboratories devised the procedure for such a determination.

This procedure makes use of a temperature gradient furnace. A holder 6-in. long with vertical cross pieces placed every ½ in., supports the glass fiber in the furnace. Each ½-in. division corresponds to a temperature change of 15 deg C within the furnace. After exposure, the portion of the fiber in the hotter region sags between supports while the section in the cooler region remains in its original position. The temperature at the first support where sag occurs—as measured by a thermocouple probe—is the sag point temperature.

By designating such parameters as the specimen diameter and the time of exposure in the furnace, the sag point can be applied universally to glasses to define a specified stage of viscosity. A diameter of 0.5 to 0.8 mm was found acceptable; within these tolerances there is little variation in the sag point temperature (table 1). Suitable fibers can be conveniently prepared by drawing directly from the melt.

The time the fiber is kept in the furnace is not critical. From 20 to 30 min gives a reproducibility within the 7-deg deviation introduced by the support interval-temperature change relationship. One of the main conveniences of the method is that it eliminates the necessity for observations during the time of test, which

TABLE 1. *Relationship between fiber diameter and sag point*

Diameter	Sag point
mm	°C
0.50 to 0.84	650
.52 to .69	650
.50 to .60	657
.55 to .70	657
.62 to .76	650

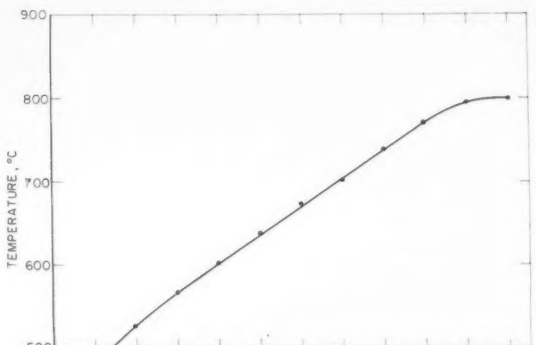

Graph showing the temperature gradient within the furnace used in determining the sag point of glass.

TABLE 2. *Temperatures of reference points of several optical glasses*

Glass type	Temperature of			b-a	c-a
	Deformation point a	Sag point b	Softening point c		
	°C	°C	°C		
BSC 511	580	655	701	75	121
BSC 517	604	653	729	49	125
LC 523	590	629	702	39	112
BaC 541	640	650	737	10	97
BaC 5725	664	697	753	33	89
BaC 574	670	718	752	48	82
BaC 617	692	731	785	39	93
CF 529	495	546	641	51	146
F 620	477	515	592	38	115

A glass fiber on a special platinum holder is inserted into a temperature gradient furnace. The temperature at which the fiber sags has been defined as a reference point in melting glasses.

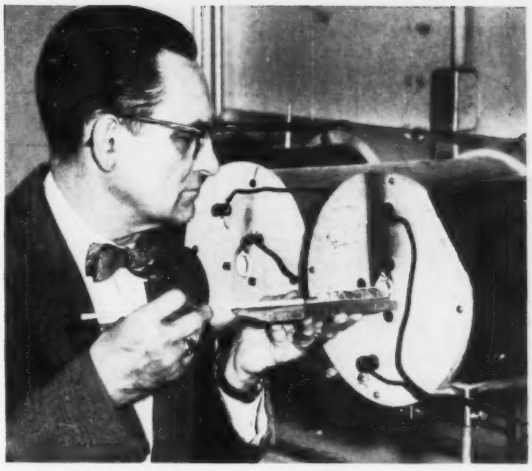

are usually a part of other reference-point determinations.

The sag point makes it possible to specify more fully the properties of different glasses. Not only do reference points, such as softening and deformation points, occur at different temperatures for different glasses, but the interval between these two extreme points also varies as does the position of the sag point, within that interval (table 2). It is therefore not sufficient in describing the physical properties of a glass to specify only one point. For example, glasses which have the same deformation point will, in all probability, have different softening and sag points. The ease and rapidity with which the sag point can be determined make it ideal for use in representing temperature-viscosity relations.

The technique for determining the sag point also indicates the success with which large pieces can be cooled without crystalization. When the fiber is removed from the furnace, if crystals have grown to the sag point from the hot end, a relatively high rate of crystal growth is indicated. Such a composition would be difficult to cool as a homogeneous glass in slabs ½-in. thick or more. On the other hand, the difficulties involved in obtaining homogeneous glasses decrease the farther the crystals appear from the sag point. A fiber emerging from the furnace with a well-defined sag point and no crystals appearing anywhere along its length would indicate the best possibility of producing a stable glass in large amounts.

[1] Determination and use of the sag points as a reference point in the heating of glasses, *by S. Spinner, G. W. Cleek, and F. H. Hamilton, J. Research NBS* **59**, 227 (1957) *RP2791.*

Photographic Determination of Reaction Rates

A TECHNIQUE for measuring the rate at which a solid surface is attacked by a corrosive gas has been developed at the Bureau. The procedure employs time-lapse photography of the reacting solid so that a permanent record of the reaction's progress is obtained at specified time intervals. From the photographs, an accurate measure of the dimensional changes and thereby the rate of change of mass of the sample can be obtained. Besides being rapid and simple, this method has the additional advantage of being applicable to any of a large number of gas-solid reactions. Developed by J. D. McKinley of the high temperature processes group of the Temperature Physics Section, the method resulted from a program of experimental and theoretical studies of reaction rates,[1] supported by the Chemistry Branch of the Atomic Energy Commission.

Few studies of gas-solid reactions involving volatile products have been conducted even though reaction-rate measurements for such systems provide valuable information on the mechanism of corrosion. At the high temperatures encountered in these studies, severe experimental complications arise. The time-lapse photographic method offers a convenient solution to many of these problems. Recently the very rapid reaction between nickel and chlorine was studied at the Bureau utilizing the technique.

The reaction of nickel with chlorine to form gaseous nickel chloride was observed over a temperature range of 1,100° to 1,700° K. The reaction was carried out in a cylindrical Pyrex vessel which can be viewed

The rate at which gas attacks a wire specimen is determined photographically. The reaction takes place in the two-armed cylindrical vessel in the line of vision of the scientist. Through a window in one arm the temperature is being measured with an optical pyrometer. The apparatus on the table controls this temperature by regulating the current sent through the wire. The camera is focused on the sample through a window in the other arm. The camera is triggered at regular intervals by a microswitch which is operated by a synchronous motor.

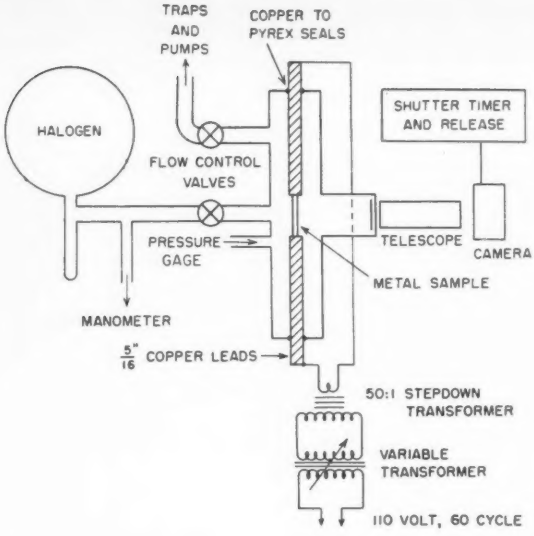

Schematic drawing showing the experimental setup employed to observe gas-solid reactions. The use of time-lapse photography permits even very rapid reactions to be studied.

through windows in two side arms at right angles to each other. The reaction vessel is designed for evacuation to pressures as low as 10^{-6} mm of mercury. The desired temperatures are obtained by mounting the sample, which takes the form of a cylindrical wire, between copper electrodes so that it can be electrically heated. An optical pyrometer focused on the sample through one of the side-arm windows allows this temperature to be accurately measured.

Time-lapse photographs are taken through the other side-arm window. Illumination is provided by a parabolic reflector lamp or by radiation from the sample, and magnification is produced by a lens system which gives a film image of the sample eight times actual size. A microswitch operated by a synchronous motor releases the shutter and advances the film at regular intervals.

In the nickel-chlorine experiments, chlorine from a high-pressure reservoir flowed through the apparatus at various constant pressures between 0.1 and 0.5 mm of mercury. Ten or fifteen exposures taken at 15- or 30-sec intervals established that the rate of change of sample diameter, and therefore the rate of reaction, is linear in time. An analysis of the photographically obtained data revealed that the reaction rate is proportional to the chlorine pressure and extremely rapid —at least 1 out of every 5 gas molecule collisions with the surface leads to a reaction.

Since the photographic method does not depend on any chemical or physical properties of the reactants, it offers several conveniences. For example, surface temperature measurements are made at the same spot upon which the camera is focused. This eliminates not only the problem of maintaining a large surface at a uniform high temperature but also that of measuring the area of reacting surface. With this method of observation, the gas and metal surface may also be heated independently, and maintained at either the same or different temperatures.

[1] *For further technical details, see* Kinetics of the reaction between nickel and chlorine above 1,100° K. *by J. D. McKinley, Jr., and K. E. Shuler, Proceedings of the XVI Congress of Pure and Applied Chemistry, Paris (1957).*

Intercomparison of Light Standards

THE BUREAU, together with six other national standardizing laboratories, recently participated in an intercomparison of light standards conducted by the International Bureau of Weights and Measures at Sèvres, France. The results indicate that the United States standards are within a few tenths of 1 percent of the averages of those of the other participating laboratories. In addition to the United States, those countries represented were France, Great Britain, Germany, Russia, Canada, and Japan.

Establishing and maintaining the standards by which luminous intensity and luminous flux—that is, the total luminous output of a light source—can be measured, are among the basic functions of the Bureau. The Bureau calibrates and issues the photometric standards that are relied upon by the lighting industry, State and city governments, industrial and commercial laboratories, and universities. These standards are used to rate all types of lamps uniformly and consistently with the national and international units now in effect. The Bureau also sample-tests all of the incandescent, fluorescent, and photoflash lamps purchased by the Federal Government.

Since 1948, standards for luminous intensity and luminous flux have been calibrated in terms of the candle, also called the "candela" in some countries, and the lumen. In 1950 these units were defined by Federal law [1] as follows: (1) "The candle . . . is one-sixtieth of the intensity of one square centimeter of a perfect radiator, known as a 'black body',[2] when operated at the temperature of freezing platinum" (2,042°K); (2) "The lumen . . . is the flux in a unit solid angle from a source of which the intensity is one candle."

The standards maintained by the Bureau, which represent the national photometric units of the United States, are periodically intercompared with similar standards of other countries. Intercomparisons with

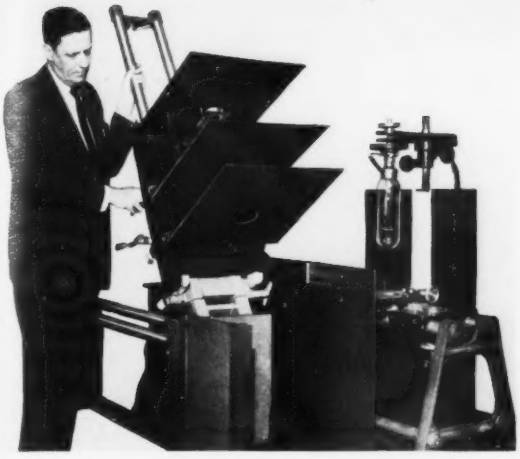

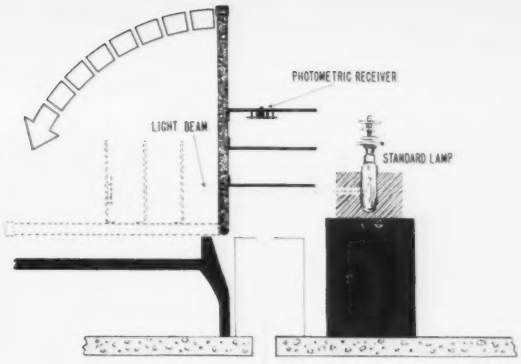

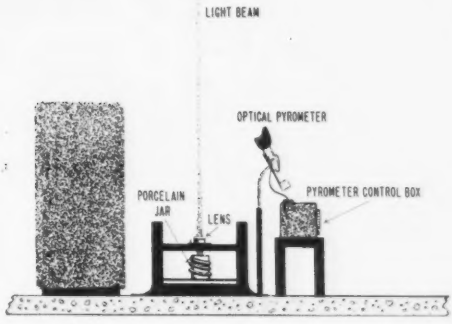

Upper right: **Apparatus, installed on two floors, used to calibrate national standards of candlepower. Diagram of equipment on upper floor (photo above) shows a photometric receiver in position to receive illumination, focused by lens on lower floor, from a black body radiator contained in a porcelain jar (photo at right). When the bar holding the photometric receiver is returned to a horizontal position, the photometric receiver is illuminated by a standard lamp. Measurements of the two illuminations are then compared. The standard lamp in the photo above is used to calibrate the lamps intercompared with other countries. An optical pyrometer, shown at right, has been turned out of the optical path. This pyrometer is used to monitor the preheating of the black body.**

lamp laboratories in this country, which are made regularly, insure uniformity in the United States, while the international intercomparisons insure uniformity throughout the world.

The recent work at the International Bureau of Weights and Measures involved intercomparisons of photometric units for lamps of various color temperatures. With the average of all participating laboratories being taken as unity, the values of the United States units at these color temperatures were: (1) 1.0031 for the candle at 2,042°K; (2) 1.0089 for the candle at 2,353°K; (3) 0.9995 for the lumen at 2,353°K; and (4) 0.999 for the lumen at 2,788°K.

Further cooperation among the various national laboratories is needed in order to reduce the spread in the values of the units. Toward this end, the Bureau is currently investigating its value for the candle at 2,353°K, and plans also to investigate its value for the candle at 2,042°K. The results thus far indicate that the final value for the candle at 2,353°K as maintained at the Bureau will be much closer to the mean of the participating laboratories than is indicated by the 1.0089 value listed above. In addition, the Bureau is setting up the primary standard for recalibration of its basic candlepower standards; also, recalibrations of the other types of standards of light in terms of these basic standards are planned.

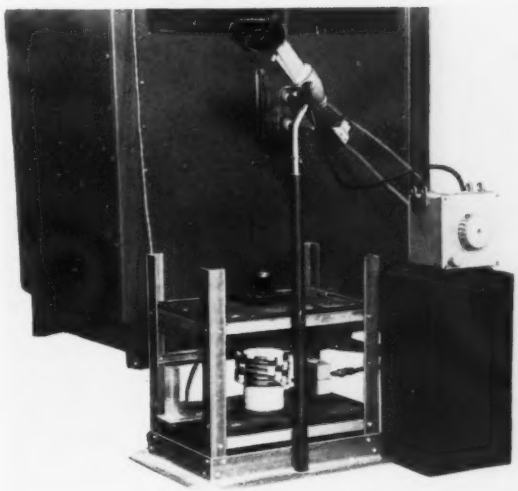

[1] *Public Law 617, 81st Congress.*

[2] *A black body is defined as a surface or body which completely absorbs all radiant energy of any wavelength falling upon it, no energy being reflected or transmitted.*

INTERFRO

for measuring gge-

MORE RAPID and convenient measurement of the parallelism of opposite faces of gage blocks is made possible by an interferometer [1] designed by J. B. Saunders of the Bureau. The instrument is adjusted by a few simple and stable controls, and the angle between the gage-block surfaces is read directly from a calibrated scale.

Use of the interferometer is expected to improve efficiency of gage-block calibration in a wide range of industries where the blocks serve as reference standards for high-precision manufacturing operations. For a growing number of processes, as in the making of machine tools, ball bearings, and missile control mechanisms, test gages for dimensional control must be accurate to within 1/100000 of an inch; and the gage blocks used in checking the accuracy of the gages must be more accurate still. The use of interferometers permits the gage blocks themselves to be measured with errors of less than a small fraction of a wavelength of the light used.

The present instrument was developed as part of a program whose goal is a substantial increase in the accuracy of dimensional standards for industry. In view of the industrial importance of this program, a group of private firms has supplemented the Bureau's congressional appropriation with additional funds to help support the necessary research.[2] Among the previous results of this work is an interferometer for comparing the linear dimensions of gage blocks to an accuracy of 1 part in 10,000,000.[3]

As in other interferometers, the basic principle utilized in the present instrument is that if 2 beams of light from the same source travel along different paths and then come together again, they will form a pattern of interference fringes, the number of fringes depending on the difference in optical path length. Usually, the 2 beams are reflected from different surfaces, so that the fringes give information about the relative position of the 2 surfaces. However, the application of the interference principle here is somewhat more complex.

Looking through the eyepiece, one sees 2 separate interference patterns, one for each of the gage-block surfaces being compared. Each pattern is formed by the interference of light rays reflected from different parts of the same surface, a result obtained by using a double-image prism. If the 2 block surfaces are parallel, the fringe patterns are also parallel; otherwise the 2 sets of fringes are inclined by an amount that depends on the angle between the surfaces. However, by placing a glass wedge in the path of the rays and rotating it to the correct position, the fringe patterns may be made parallel. The angle between the 2 surfaces can then be read directly from a suitably calibrated scale attached to the wedge.

In previous applications of interference to the measurement of gage-block parallelism, the procedure has been to wring the block onto an optically flat surface and to measure by interferometric means the angle between the upper surface of the block and the exposed portion of the optical flat. The wringing involves contact with the hand, which raises the block's temperature and may entail a long wait for temperature equilibrium to be established; it also causes undesirable wear of the gage-block surfaces.

The present instrument avoids both of these difficulties by measuring the angle between the opposite faces of the block by a direct comparison of the 2 faces. Although its optical arrangement is more complex, pre-

FROMETER

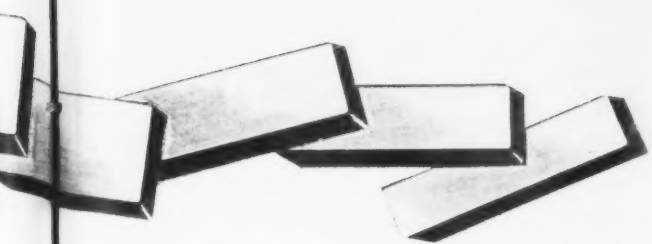

gge-block parallelism

liminary tests show not only that it can be operated more easily, but that the operating procedure can be reduced to a simple routine.

In outlining how the instrument works, it is convenient to proceed in 3 stages, describing: (1) The principal components and their arrangement; (2) the basic manner of operation; and (3) the refinements that make possible a direct reading of the angle.

Interferometer for testing parallelism of gage-block surfaces. Principal components are the light source at end of collimating tube (upper right), viewing tube with micrometer eyepiece through which scientist is looking, double-image prism in triangular housing (upper part of instrument), perforated plate on which gage block rests (visible through open door), circular glass wedge mounted just below gage-block plate (not visible), and a right-angle prism at bottom of instrument (not visible).

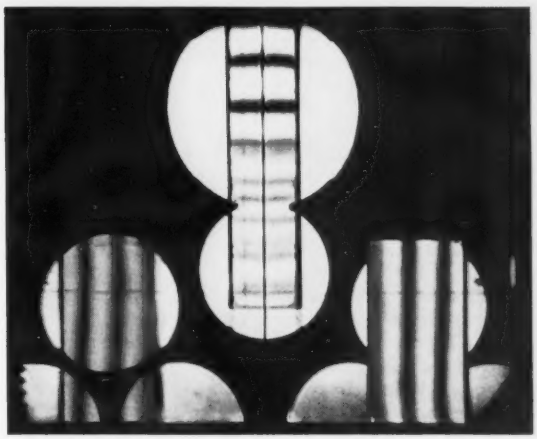

Portion of field as seen through interferometer eyepiece. *Lower right:* Upper surface of gage block. *Lower left:* Lower surface of block seen through perforations in mounting table. Fringes on center plate are used in calibration process.

Principal Components

The principal optical components are a double-image Kösters prism and a right-angle prism. The double-image prism is made by taking two 30–60–90° prisms, depositing a semitransparent layer of aluminum on a face of one of them, and cementing the two together with the aluminized face on the inside. The resulting unit is a 60–60–60° prism which is "split" down the middle by the semitransparent layer.[4] The right-angle prism is used for its well-known property that a ray of light entering through the base (face opposite right angle) along any line perpendicular to the 90° edge will emerge, after 2 internal reflections, along a path exactly parallel (and opposite) to its original direction.

In describing the arrangement of the various components, it is useful to refer to the "central plane", which contains the aluminized layer; and to the "transverse plane", which is perpendicular to the central plane and passes through the center of the double-image prism.

The double-image prism is mounted with its base (face bisected by the aluminum film) downward and horizontal; and the right-angle prism is about a foot directly below with its base upward and its 90° edge in the transverse plane. The gage block to be measured is supported on a perforated plate between the 2 prisms. It is placed to one side of the transverse plane so that its upper and lower surfaces (the angle between which is to be measured) are approximately horizontal and are bisected by the central plane.

Light from a point source is collimated into a parallel beam, the collimator axis being normal to one of the upper surfaces of the double-image prism. A viewing tube, containing an objective lens and a micrometer eyepiece, has its axis normal to the other upper surface.

Basic Operation

The parallel beam from the collimator passes through the double-image prism to the semitransparent layer, where each of its rays is divided into 2 parts; one continues ahead to the opposite face and is internally reflected straight downward; the other part is bent back to the face through which it entered and is there reflected downward. The 2 emerging rays (which derive from a single original ray) are symmetrical with respect to the central plane.

Some of the rays on one side of the transverse plane strike the top surface of the gage block and are reflected back to the prism. If the surface is perpendicular to the rays, both members of a symmetrical pair are reflected back along their paths to the semitransparent surface. Here each ray is again split, and half of one combines with half of the other to emerge along the same line towards the viewing tube.

Similar remarks apply to rays on the other side of the transverse plane, except that these pass through the right-angle prism and emerge vertically upward. Some of these strike the lower surface of the gage block. If this is perpendicular to the rays, a given symmetrical pair will be reflected back along their paths and, by the process described, combine to form a single ray moving toward the viewing tube.

Rays that do not strike the gage block are internally reflected in the right-angle prism, each ray of a pair moving up along the path by which the symmetrical ray had descended. As before, the 2 rays are recombined at the aluminized surface and proceed to the viewing tube where they form the background of the field of view.

The first step in using the instrument is to adjust the control knob, if necessary, to orient the right-angle prism so that its base is perpendicular to the rays. When this is the case, all light paths (for rays that do not strike the gage block) are equal and no interference fringes appear in the background of the field. (More correctly, one sees a small portion of a very broad fringe; in the limiting case, the width of this fringe would be infinite.) With a second control adjustment, the mounting plate on which the gage block rests is oriented so that the upper block surface is also perpendicular to the rays, as indicated by the absence of fringes in the part of the field corresponding to the upper surface.

The appearance through the eyepiece of the lower surface of the block now indicates the size of the angle, if any, between it and the upper surface. If the surfaces are parallel, the lower one is also perpendicular to the rays, and no fringes appear; and the more fringes the greater the angle between the surfaces.

It should be noted that the instrument measures one "component" of the inclination at a time. That is, any sufficiently small inclination (such as occurs here) can be thought of as obtained by rotating the surface (from the position of zero inclination) successively about 2 perpendicular axes lying in the surface. The instrument measures only that part of the inclination corresponding to rotation about the line in which the surface intersects the central plane. In the basic instrument as described thus far, the fringes will be parallel to this line. To measure the other component of the

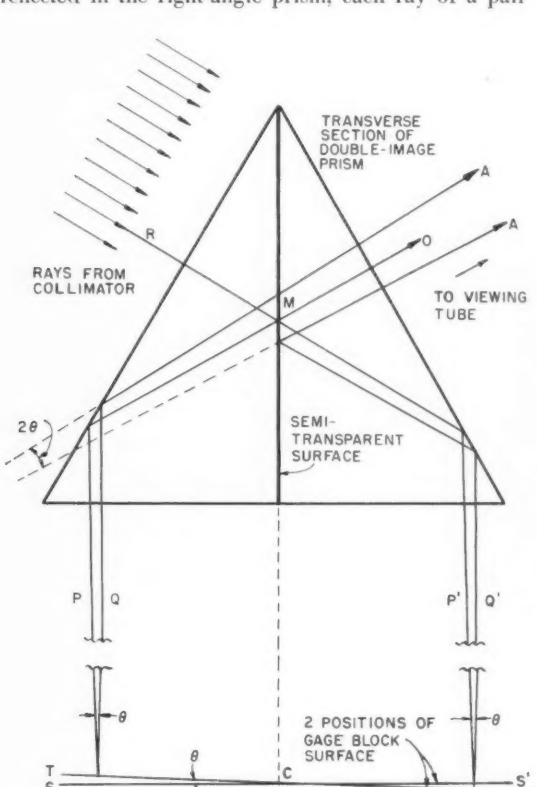

Diagram to illustrate the formation of interference fringes in the instrument recently developed for testing the parallelism of gage-block surfaces. (Only the basic principle is illustrated; refinements that permit a direct reading of the inclination of a surface are not taken into account.) A ray, R, enters the double-image prism and is split into 2 components at point M of the semitransparent surface; after internal reflection, the 2 rays emerge along symmetrical paths P and P′. If reflecting surface SS′ is perpendicular to these rays, they return along the same paths to M where half of each ray combines with half of the other to form ray MO. Since both rays traverse equal optical paths, no interference fringes are formed. However, if SS′ is rotated to the position TT′, the rays return along Q and Q′ and emerge in the directions A and A′. The lengths of the 2 paths now differ. If they differ by an even number of half-wavelengths of light, the rays reinforce each other when brought together by the lenses of the viewing tube; if by an odd number of half-wavelengths, the rays cancel, producing darkness. The amount of the difference depends on the distance of the symmetrical rays from the line through the center C of the reflecting surface and perpendicular to the plane of the diagram. Hence, the fringes of light and darkness run perpendicularly to the plane of the diagram. If the surface had been rotated, instead, about the axis SCS′, no fringes would be produced, since the changes in path length would affect both members of a symmetrical pair of rays equally. Thus the instrument measures one component of the inclination at a time; to measure the other component, the gage block is rotated through 90°.

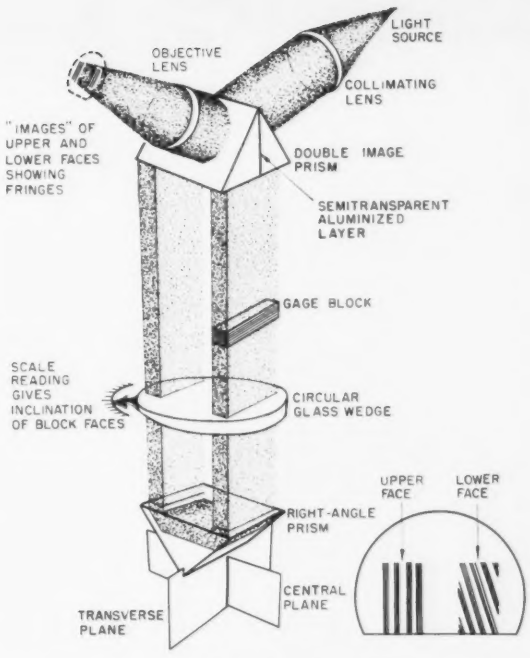

Pictorial diagram of the interferometer for measuring the deviation from parallelism of the opposite faces of a gage block. The light from the collimator is split into 2 beams by the semitransparent layer, and parts of both beams strike the upper face of the block. If the block is adjusted so that the upper face is perpendicular to the beams, the latter are reflected back along their paths and recombine at the semitransparent surface. If the glass wedge is ignored for the moment, the 2 beams travel the same distance and so do not form interference fringes. However, the 2 halves of the double-image prism have been twisted slightly, so that a permanent set of fringes is introduced. When the upper face is now set perpendicular to the semitransparent surface, these fringes will also be perpendicular to that surface. At the same time, parts of both beams reach the lower face of the block by way of the right-angle prism. If this face is parallel to the upper one, a set of fringes parallel to those of the upper face is seen. If the faces are inclined, the fringes from the lower face are rotated as shown in the insert. The glass wedge introduces a variable difference in the paths of the 2 beams, and if it is turned the correct amount, will compensate for the difference in path due to the inclination of the block faces. When compensation occurs, the 2 sets of fringes are parallel. It is therefore possible to calibrate the scale associated with the wedge so that the inclination can be read off directly. For simplicity, rays that do not strike either face of the block (and form the background of the field of view) are not shown.

inclination, the block is rotated through 90°. In either case, if 2.6 fringes are observed, for example, the component of the inclination is equal to $2.6\lambda/2L$ radians, where λ is the wavelength of the light and $2L$ is the dimension of the block perpendicular to the central axis.

Direct Reading of the Inclination

Two additional features permit a direct reading of the inclination. Without changing the basic optics of the instrument as described above, this results in an important gain in speed and convenience.

First, while the cement between the 2 halves of the double-image prism is still soft, the 2 parts are twisted slightly with respect to each other. The twist—a rotary, sliding motion of the 2 surfaces separated by the cement—amounts to only a few seconds of arc. As a result, the 2 beams emerging from the base on either side of the central plane are no longer exactly symmetrical; however, each remains parallel to the central plane.

The effect of this can be seen by supposing the instrument to be adjusted in the manner described above. When the upper face of the block is set perpendicular to the rays it now exhibits a permanent set of fringes perpendicular to the central plane. If the lower block surface is parallel to the upper one, it will exhibit a set of fringes parallel to those of the upper surface. However, if it has a component of inclination about a horizontal axis in the central plane, the fringes are turned through an angle that depends on the size of that component. This angle can be measured with the help of the micrometer eyepiece, and from the angle one can calculate the inclination.

Direct reading of the inclination can now be obtained with the help of a circular glass disk cut from a glass plate whose faces are inclined to each other. This circular wedge, placed between the gage block and the right-angle prism, can be rotated about a vertical axis and its angular position is indicated on a circular scale.

The wedge introduces a controllable amount of difference in the optical paths of the 2 rays of a symmetrical pair. When the planes of the wedge are perpendicular to the central plane, the 2 paths are changed by equal amounts and the fringe pattern is unaffected. In other positions of the wedge, the 2 paths are affected differently; and by suitably adjusting the position it is possible to compensate for the inclination of the lower block surface. When this is done, the fringes from the lower surface have the same appearance as those from the upper surface. Thus the angular position of the wedge required to produce compensation depends on the amount of inclination; so that a direct reading of the inclination is achieved by a suitable calibration of the associated scale. Monochromatic light must be used in the calibration procedure; thereafter, since the instrument operates on a null principle, it can be used with white light without materially reducing the precision.

---

[1] *For further technical details, see* The parallel testing interferometer *by J. B. Saunders* (in preparation).

[2] *The firms that have supported the development of the present instrument are Dearborn Gage Co., The DoAll Co., E. I. du Pont de Nemours & Co., Greenfield Tap and Die Corp., Hughes Aircraft Co., Pratt & Whitney Co., Inc., The Sheffield Corp., The Taft-Peirce Manufacturing Co., The Timken Roller Bearing Co., United Aircraft Corp., and the Van Keuren Co.*

[3] Gage-block comparator, *NBS Tech. News Bul.* **40,** *176 (December 1956).*

[4] Construction of a Kösters double-image prism, *by J. B. Saunders, J. Research NBS* **58,** *21 (January 1957) RP2729.*

Electrical Characteristics of Printed Circuit Panels

THE BUREAU has been investigating the electrical characteristics of several types of copper-clad laminates for printed circuit applications [1] as part of its program for determining the properties of materials. These laminated panels consist of a central core of insulating material with thin-sheet copper bonded to one or both sides. Under a program sponsored by the Navy Bureau of Ships, D. S. Hoynes of the Bureau's electronic engineering laboratory has studied their current-carrying capacity, electrical resistivity, and dielectric properties.

Designers of military and industrial electronic equipment are making increased use of printed circuits because of their simplicity, economy, and adaptability to mass-production methods. Design and application of printed circuit panels is, in most cases, a straightforward matter since the conductors can usually carry more current than is encountered in most electronic circuits. Occasionally, however, because of space limitations, narrow or closely-spaced conductors must be used. It then becomes necessary to know with some degree of certainty whether a particular conductor can fulfill its current-carrying requirements. Because information of this type has not been generally available, the Bureau undertook a study of the characteristics of printed circuit panels under various conditions of use.

Temperature Rise Measurements

To obtain a general temperature-behavior pattern for the current-carrying capacity of printed circuit conductors, a large number of measurements were made, under different conditions of use, on various lengths and widths of conductors bonded to a variety of materials. The curves derived from the measurements showed that cross-sectional area is a dominant factor in the ability of a conductor to carry a given current for a particular temperature rise, especially for the usual copper thickness of 0.00135 in. (1 oz) and 0.0027 in. (2 oz). As might be expected, heavier coppers (0.004 in.), appear capable of carrying somewhat less current, and thinner coppers (0.00067 in.) somewhat higher current, for a given cross-sectional area than do medium-weight coppers.

Another factor affecting the temperature-current relationship is the thickness of the laminate core material. Core materials about 1/32-in. thick showed some reduction in current-carrying capacity compared with heavier cores. When a solid copper backing was used, the same type of material showed a higher current-carrying capacity. For the usual 1/16-in. core thickness, only small differences could be noticed between single-clad and double-clad laminate panels. Variations in ambient temperature also appear to have little effect on the temperature rise above ambient due to a given current.

A reduction in current-carrying capacity of about 15 to 20 percent for a given temperature rise was noted for samples coated with a protective plastic material. Such samples were less able to dissipate the heat generated in the copper conductor. Although in most samples the resistance of a particular conductor is actually decreased by dip soldering, an additional reduction in current-carrying capacity up to about 30 percent was noted in many dip-soldered samples. This has been attributed to changes in the bond characteristics of the materials.

Surface Resistivity

Test samples of metal-clad laminates were subjected to a temperature of 70° C and 95-percent relative humidity for a period of 2,000 hr to determine the effects of various protective coatings on the surface electrical resistivity of the core material. Seven groups of XXXP-composition phenolic laminates and one of the epoxy glass-mat type were included in this test. The coatings included various epoxy resins, microwax, varnish, and silicone compounds. The variation in surface resistivity for the coated samples was generally much higher than for uncoated control samples.

Little variation was found between dip-soldered and nondip-soldered samples. Although no set pattern has been established that could not be ascribed to normal variations in the samples, a slight trend toward higher surface resistivities was detected for the dip-soldered samples.

In comparing the surface resistivity curves for the coated samples with those for the uncoated controls, little or no improvement was seen in most instances for the six coating materials. Considerable variation in the resultant surface resistivity beyond that recorded for the control samples was the rule rather than the exception. Additional variations were noted in the behavior of a particular coating material on different core materials.

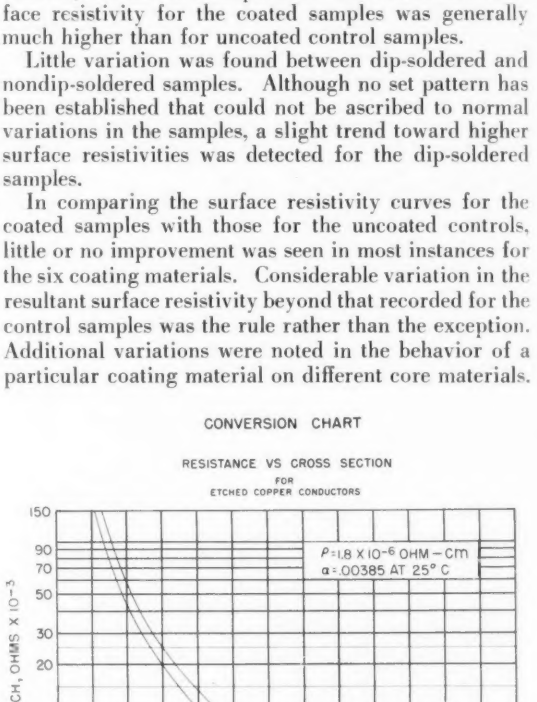

Dissipation Factor

Measurements were made over a frequency range of 10^{3} to 10^{7} cps on the dielectric properties of a group of 16 metal-clad laminates. Individual families of curves for each laminate were developed for dissipation factor and dielectric constant at −30° C, +23° C, and +100° C. Additional measurements were made at 150° C and 200° C on materials that might be expected to be useful at these higher temperatures.

With the exception of one sample, all of the phenolic-base materials showed a general reduction in dissipation factor with an increase in temperature at a frequency of 10^{6} cycles. However, considerable variation in dissipation factor was observed for the entire phenolic group at the lower frequencies, particularly at the 100° C temperature level.

Two samples of the epoxy-glass mat type laminates also showed a variation in characteristics similar to the phenolics. However, at temperatures of 100° C or less, both samples showed less change in dissipation factor than those of the phenolic group over the entire frequency range.

Considerable differences in behavior were exhibited by the two glass-melamine G–5 samples tested. In one sample, the dissipation factor was influenced to an extreme degree by the test temperature. At 100° C, the dissipation factor was so high that it was impractical to make a determination with the existing equipment. The second sample showed characteristics similar to these of the phenolics with respect to temperature, but had a dissipation factor of less than 0.02 at 10^{6} cycles. This value compares well with the epoxy samples tested.

For one sample of silicone G–7 material, the dissipation factor at 10^{6} cycles was 0.02 or less at temperatures up to 100° C but was influenced to a marked degree at lower frequencies.

The polytetrafluoroethylene-glass mat sample had the lowest dissipation factor of any of those tested in the group. Some variations did occur at the various temperature levels, but they are relatively slight considering the temperature range. At −30° C, the dissipation factor was nearly constant over the entire frequency range.

The nylon-base phenolic N–1 material showed good stability at the lower temperatures. At the higher temperature of 100° C, the dissipation factor increased as the frequency increased.

Dielectric Constant

Determinations of the dielectric constant of the various core materials showed that this factor increased generally at higher temperatures. The outstanding exception was the polytetrafluoroethylene-glass mat material, which showed the opposite trend.

In the phenolic group, the dielectric constant tended to be somewhat lower for the XXXP materials than for the XXP and XXX materials. At 10^{6} cycles, an over-all average for the XXXP materials tested was about 4, while for the XXX and XXP materials the dielectric constant averaged about 5. Both of the epoxy-base samples tested had dielectric constants at 10^{6} cycles ranging between 5 and 6 at temperatures below 100° C. Above this temperature both samples showed increases to a value above 6.

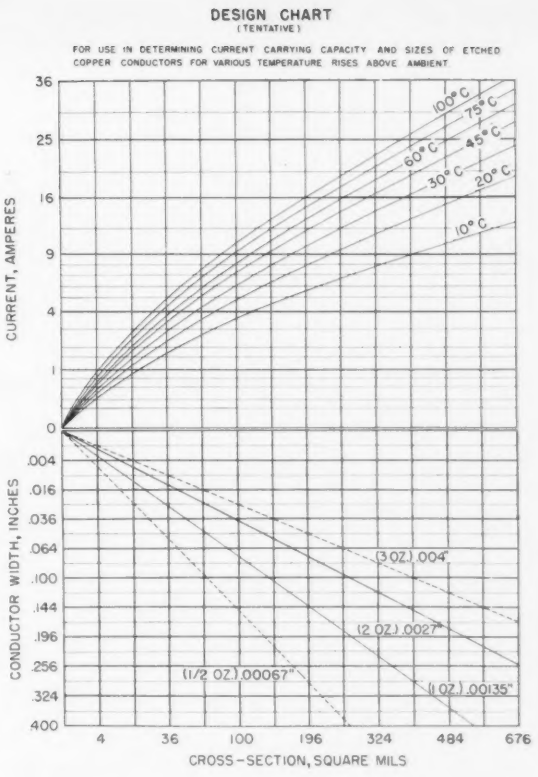

Design Charts

One result of the work is a tentative design chart to aid in estimating temperature rise above ambient versus current for various cross-sectional areas of etched copper conductors. It is intended for use primarily with XXXP and epoxy-glass materials of 1/16-in. to 1/8-in. thickness and copper thickness of 0.00135 in. (1 oz), and 0.0027 in. (2 oz). Conductor surface area is assumed to be relatively small compared to the adjacent free panel area. The curves, as presented, include a nominal 10-percent current derating to allow for variations in etching technique and conductor-width estimates under optimum conditions of use. For general application, an additional current derating of up to 50 percent should be allowed in order to compensate for different panel and copper thicknesses, the use of dip-soldering techniques, and coatings.

For single conductor applications the chart can be used directly for determining conductor widths, conductor thickness, cross-sectional area, and current-carrying capacity for various temperature rises.

For groups of similar parallel conductors, if closely spaced, the temperature rise may be found by using an equivalent cross section and an equivalent current. The equivalent cross section is equal to the sum of the cross sections of the parallel conductors, and the equivalent current is equal to the sum of the currents in the conductors.

For applications where etched coils are to be used, the maximum temperature rise can be obtained by using an equivalent cross section equal to $2n$ times the cross section area of the conductor, and an equivalent current equal to $2n$ times the current in the coil where n is equal to the number of turns.

A conversion chart has also been developed showing resistance per linear inch versus cross section for etched conductors, applicable where the IR drop in a conductor may be the primary consideration instead of temperature rise.

[1] *For further technical information, see* Characteristics of metal-clad laminates, *by D. S. Hoynes, Electrical Manufacturing,* **59** *no. 4, p. 110 (April 1957).*

Photometric Determination of Tungsten in Steel

TUNGSTEN in the range of 2 percent or less is finding increasing application as an alloying element in ferrous metallurgy as it provides improved durability, hardness, and high-temperature properties to steels. Typical alloys incorporating tungsten include "nondeforming" die and chisel steels, age-hardening alloys, tool steels, and certain types of stainless steels.

In producing steels for specific uses, accurate quantitative analysis is necessary to control the manufacturing process. Rapid spectrographic procedures can be used for this purpose only if carefully analyzed reference standards of the steels are available for comparisons. However, satisfactory chemical methods for determining small amounts of tungsten in the presence of other elements normally encountered in iron metallurgy have been lacking. To meet this need, L. A. Machlan and J. L. Hague of the Bureau have developed a direct photometric method [1] for precisely determining minute quantities of tungsten in steel. The technique has been used to analyze low-tungsten steel specimens for distribution to industry as NBS standard samples.[2]

The method involves the use of dithiol reagent (1,2-dithiol-4-methylbenzene), which offers several advantages over previous techniques for the determination of small quantities of tungsten in steels. With dithiol, potential metal interferences are eliminated by separation of metal complexes formed with the reagent. Following the removal of these interfering elements, a clear blue tungsten-dithiol complex is formed. After extraction in butyl acetate, the absorbancy of this complex is measured in a photometer to determine the percentage of tungsten present. A single determination can be completed in several hours; a group of 6 or 8 can be made in a day.

Determination of minute quantities of tungsten in steel at the analytical laboratory. Measuring the optical absorbancy of a tungsten-dithiol complex in a colorimeter is the final experimental step in the Bureau-developed method; the actual tungsten content is obtained from this measurement by reference to a chart or table.

In the usual cinchonine gravimetric procedure, iron and molybdenum retard the complete precipitation of minute amounts of tungsten. When thiocyanate reagent is used in the photometric analysis of tungsten, positive errors are encountered from molybdenum or vanadium; if hydroquinone is used, titanium and niobium cause inaccurate results.

As the first step in the dithiol procedure, the metal sample is dissolved in aqua regia. A sulfuric-phosphoric-perchloric acid mixture is then added. The resulting mixture is heated until some sulfuric acid fumes are given off, signifying complete solution of the steel.

When dithiol is added to the solution, it combines with any molybdenum present to form a complex which is removed by chloroform extraction. Copper also unites with the dithiol, forming a black precipitate and preventing complete molybdenum extraction in the chloroform layer. Since this copper precipitate apparently occludes some of the molybdenum, the solution is filtered through glass wool to remove the interfering precipitate. If there is molybdenum in the original metal, the dithiol and chloroform steps are repeated. The molybdenum must be removed completely, because if allowed to remain it will impart a green color to the final blue solution and interfere with the photometric analysis.

The solution is then heated to remove sulfur dioxide, which inhibits tungsten color development, and to eliminate any remaining chloroform, which would increase the volume of solvent used to extract the dithiol complex.

Before the tungsten-dithiol complex will form, the tungsten must be reduced with stannous chloride in the presence of hydrochloric acid. After this step, dithiol is again added, this time to form the bright blue tungsten-dithiol complex, which is extracted in butyl acetate. To check for the possible incomplete extraction of molybdenum, the optical absorbancy of the tungsten-dithiol complex in the butyl-acetate layer is measured in a colorimeter at two wavelengths, 635 and 720 mμ. Any change in the ratio of the 635 to 720 mμ absorbancy values indicates this contaminant. The actual tungsten content of the sample is then determined by reference to a chart or table. Experiments using a second extraction with the acetate show that the tungsten-dithiol complex is more than 99-percent removed by one separation.

Fifteen elements—antimony, arsenic, bismuth, chromium, cobalt, lead, manganese, mercury, nickel, platinum, rhenium, selenium, silver, tin, and vanadium—were investigated as potential interfering agents in the determination of tungsten; they neither hindered molybdenum elimination nor blocked tungsten color development.

An accuracy of 0.005 percent was found for samples containing between 0.5- and 0.05-percent tungsten while an accuracy of 0.001 percent was indicated for samples with less than 0.05-percent tungsten. However, as the absorbancy of the tungsten-dithiol complex varies with temperature (about 0.2 percent per degree), measurements should be taken within a 5-degree range to obtain this accuracy.

[1] *For further technical information, see* Photometric determination of tungsten in steel and titanium alloys with dithiol, *L. A. Machlan and J. L. Hague, J. Research NBS*, **59**, *415 (1957) RP2812.*

[2] *Over 550 different certified standard samples of chemicals, ores, ceramics, and metals are distributed by the Bureau. Additional information may be obtained from* Standards samples and reference standards, *NBS Circular 552 (2d ed.), Superintendent of Documents, U. S. Government Printing Office, Washington 25, D. C. (25 cents).*

Torque Values of Spring Wire Recorded

THE BUREAU, in work sponsored by the Army Ordnance Corps, Springfield Armory, has been investigating the effect of metallurgical variables on the properties of spring wire. Because the wire from which helical extension or compression springs is wound is stressed in torsion, a means was sought for measuring the torsional properties easily and accurately. Consequently, an apparatus was constructed that automatically records the torque-twist characteristics of wire less than 0.05 in. in diameter.[1]

Designed by H. C. Burnett and J. A. Bennett of the mechanical metallurgy laboratory, the equipment provides a rapid, easy method for determining the torsional properties of small-diameter wire. The spark recording system utilized is entirely frictionless so that even small torque values can be recorded accurately. The apparatus should be of general utility in developing more significant specifications for the spring wire used in many types of ordnance items.

The method of making the measurements is to couple the test wire in series with a larger-diameter calibrated wire and to rotate one end of the assembly. The twist in the calibrated wire is a measure of the torque and is recorded on one axis of a chart, while the twist in the test wire is recorded along the other axis.

The framework of the device is a table with two shelves clamped to the legs. A small motor and reduction gear are mounted on the table surface. The wire undergoing test, cut to a length of approximately 6½ in., is suspended from a coupling attached to the motor's drive shaft which extends through an opening in the table surface.

The bottom end of the test wire is coupled, through an opening in the middle shelf, with the measuring wire which is of larger diameter and about three times as long as the test wire. The measuring wire is held in a coupling keyed to the bottom shelf, and is spring loaded to provide a small amount of tension to both wires. To eliminate oscillations, an inverted damping cup, immersed in a pan of light oil, is fastened to the coupling at the bottom of the test wire.

A fixed helical electrode is mounted on the middle shelf. Fitted vertically inside the fixed electrode is a movable-bar electrode supported by the coupling

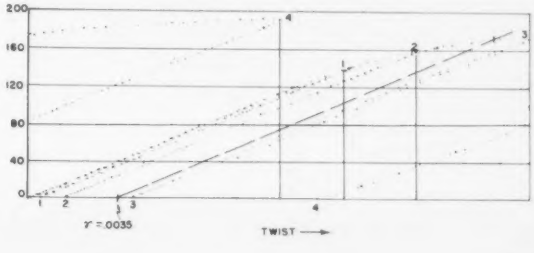

Record of the torsional characteristics of oil-tempered wire, 0.039 in. in diameter. The load is shown on the ordinate as nominal surface shear stress, 1,000 lb/in.^{2}. During this test, the test wire was alternately loaded and unloaded 4 times. The numbers 1 through 4 on the curves indicate the peak stress of each cycle. The numbers 1 through 4 along the base locate the total permanent set resulting from the corresponding cycles. The yield strength is determined at a shear strain offset of 0.0035.

Machine developed to record the torsional properties of small-diameter wire. A damping cup is being placed around the measuring wire. Motor and reduction gear assembly are mounted on the top shelf. Cylinder of heat sensitive paper has been partially cut away to show the movable-bar electrode behind the test wire suspended from a coupling. The fixed-helical electrode, mounted on the middle shelf, fits around the paper cylinder. Recording is accomplished by a spark jumping from the helical electrode on the outside of the paper cylinder to the movable-bar electrode on the inside.

between the two wires. A cylinder of heat-sensitive paper, on which the torque-twist measurements are recorded, is taped firmly around a disk attached to the top of the test wire. This paper cylinder, scaled at appropriate torque and twist values, hangs suspended between the movable bar electrode and the fixed helical electrode without touching either one. Both of the electrodes are designed with a knife edge so that the position of the spark locates accurately the point where the electrodes are closest together.

To conduct a test, the upper end of the test wire is rotated by the motor and reduction gear at an angular speed of about 100° per minute. At the same time, an interrupter and ignition coil produce sparks at 5-second intervals between the two electrodes, causing a line of small black dots to appear on the paper.

The angular deflection of the movable-bar electrode is proportional to the torque applied to the measuring wire. This deflection displaces the position of the spark vertically on the paper. The position of the spark is displaced horizontally by the twist in the test wire. It is this twist in the test wire that causes rotation of the paper cylinder relative to the movable-bar electrode. Thus, as the sparks pass through the paper from the fixed to the movable electrode, the torque-twist relationship of the test wire is recorded.

The machine fills a gap in the equipment now available for testing small-diameter wire. Its construction allows flexibility in the length of test wire and the torque range of the measuring wire. The device also has the advantages of low first cost and an absence of complicated accessories.

[1] *For further technical details, see* A recording torsion testing machine for wire, *by H. C. Burnett, ASTM Bul. (in press).*

Direct Determination of Sound Speed in Liquids

THE BUREAU has developed a simple, fast-acting, precision instrument to measure the speed of sound in nondispersive liquids—liquids in which the speed of sound is essentially independent of frequency. M. Greenspan and C. E. Tschiegg of the sound laboratory designed and constructed this instrument under the sponsorship of the Office of Naval Research. It has been used to measure the speed of sound in distilled water from 0° to 100° C with an accuracy of 1 part in 30,000.[1]

Accurate values of the speed of sound in water are required to calibrate field velocimeters [2] used in underwater sound research by oceanographers and naval engineers. Previously obtained data contain discrepancies which exceed the claimed accuracy of the measuring methods. Another questionable aspect of previous measurements is that no set of data exists which gives a smooth variation with temperature over any considerable range. Data on the speed of sound in other liquids are also important; they can be combined with density values to determine adiabatic compressibility and the ratio of specific heats. The newly developed method not only satisfies these requirements but also is adaptable to measurements in a solid medium.

The sample in which the speed of sound is to be measured is confined in a tube; the ends of this tube are plane, parallel, quartz crystals, which serve as electroacoustic transducers. If a very short pulse is impressed on one crystal (sender), then an oscilloscope connected to the other crystal (receiver) will show a series of received pulses. These pulses arise from the reverberation of the impressed sound pulse between

Left: **Measuring the speed of sound in water with a fast-acting, precision instrument. A tube (below) equipped with crystal oscillator end plates is immersed in a heated tank of distilled water. When certain coincidence conditions are satisfied between a pulse imposed on one crystal and the echo of a previous pulse, the frequency indicated on the timer at right is the reciprocal of the travel time of sound in the tube. The coincidence is observed on the oscilloscope screen in the background. From the time and the known length of the tube, the speed can be obtained by a simple L/t calculation.**

TABLE 1. *NBS measurements of the speed of sound in water at various temperatures*

Temperature	Speed
°C	m/sec
0	1402.74
10	1447.59
20	1482.66
30	1509.44
40	1529.18
50	1542.87
60	1551.30
70	1555.12
80	1554.81
90	1550.79
100	1543.41

the two transducers. The received pulses are separated by the travel time of the pulse over twice the length of the tank. This travel time divided into the total path length is the speed of sound in the sample.

The exciting pulses are derived from a sine-wave oscillator and applied repetitively to the sender crystal by a blocking oscillator. By varying the frequency of the sine-wave oscillator, a coincidence is obtained between the first received pulse corresponding to a particular electrical pulse and the first echo of the preceding electrical pulse. After amplification, this coincidence is observed on the oscilloscope screen. With this coincidence condition, the frequency, which can be measured with an electronic counter, is the reciprocal of the travel time.

From the travel time and the path length, which is known from the tube dimensions, the speed of sound is calculated. Values for the speed of sound in water were obtained at 83 temperatures between 0.14° and 99.06° C. These calculated values have been fitted to a fifth-degree polynomial.

[1] Speed of sound in water by a direct method, *by M. Greenspan and C. E. Tschiegg, J. Research NBS* **59,** *249 (1957) RP2795.*

[2] An automatic underwater velocimeter, *NBS Tech. News Bul.* **39,** *89 (1955).*

Publications of the National Bureau of Standards

Periodicals

Journal of Research of the National Bureau of Standards, Volume **60,** No. 1, January 1958 (RP2815 to RP2832 incl.), 60 cents. Annual subscription $4.00.

Technical News Bulletin, Volume **42,** No. 1, January 1958. 10 cents. Annual subscription $1.00.

Basic Radio Propagation Predictions for April 1958. Three months in advance. CRPL–D161. Issued January 1958. 10 cents. Annual subscription $1.00.

Research Papers

Journal of Research, Volume **60,** *No. 1, January 1958. 60 cents.*

RP2815. The condition of certain matrices, III. John Todd.

RP2816. Infrared study of some structural changes in natural rubber during vulcanization. Frederic J. Linnig and James E. Stewart.

RP2817. Crystal structure of barium hydrogen orthophosphate. Gordon Burley.

RP2818. A study of sampling of flame gases. C. Halpern and F. W. Ruegg.

RP2819. Pyrolysis of polyamides. Sidney Straus and Leo A. Wall.

RP2820. Some thermodynamic properties of the systems polybutadiene-benzene and polyisobutene-benzene. R. S. Jessup.

RP2821. Infrared measurements with a small grating from 100 to 300 microns. Earle K. Plyler and L. R. Blaine.

RP2822. A low-frequency annular-slot antenna. James R. Wait.

RP2823. Relation between the absorption spectra and the chemical constitution of dyes: XXIX. Interaction of direct azo dyes in aqueous solution. May N. Inscoe, John H. Gould, Mary E. Corning, and Wallace R. Brode.

UNITED STATES
GOVERNMENT PRINTING OFFICE
DIVISION OF PUBLIC DOCUMENTS
WASHINGTON 25, D. C.

OFFICIAL BUSINESS

PENALTY FOR PRIVATE USE TO AVOID
PAYMENT OF POSTAGE, $300
(GPO)

TECHNICAL NEWS BULLETIN

U. S. DEPARTMENT OF COMMERCE
SINCLAIR WEEKS, *Secretary*
NATIONAL BUREAU OF STANDARDS
A. V. ASTIN, *Director*

February 1958 **Issued Monthly** **Vol. 42, No. 2**

For sale by the Superintendent of Documents, U. S. Government Printing Office, Washington 25, D. C. Subscription price, domestic $1.00 a year; 35 cents additional for foreign mailing; single copy, 10 cents. Use of funds for printing this publication approved by the Director of the Bureau of the Budget (March 29, 1956).

Contents

	Page
Redetermination of the standard ampere	21
Impact behavior of plastics	23
X-ray penetration in lead	24
The sag point, a reference in heating glasses	26
Photographic determination of reaction rates	27
Intercomparison of light standards	28
Interferometer for measuring gage-block parallelism	30
Electrical characteristics of printed circuit panels	34
Photometric determination of tungsten in steel	36
Torque values of spring wire recorded	37
Direct determination of sound speed in liquids	38
Publications of the National Bureau of Standards	39

NBS Publications (*continued*)

Handbooks

H63. Protection against neutron radiation up to 30 million electron volts. 40 cents.

H64. Design of free-air ionization chambers. H. O. Wyckoff and F. H. Attix. 20 cents.

Publications in Other Journals

Construction and application of a class of modular functions. Morris Newman. Proc. London Math. Soc. [3] **7,** 334–350 (July 1957).

Electron scattering phenomena. L. Marton. J. Sci. Ind. Research. **16a,** No. 6, 221–230 (1957).

Frozen free radicals: The problem and the program at the National Bureau of Standards. L. T. Milliken. Capitol Chem. **7,** No. 8, 244–247 (Nov. 1957).

Hexafluorobenzene from the pyrolysis of tribromofluoromethane. M. Hellmann, E. Peters, W. J. Pummer, and L. A. Wall. J. Am. Chem. Soc. **79,** 5654 (Nov. 1957).

Inelastic scattering of 20-kev electrons in metal vapors. Lewis B. Leder. Phys. Rev. **107,** No. 6, 1569–1578 (Sept. 1957).

Measurement of voltage ratio at audio frequencies. Wilbur C. Sze. Communs. Electronic. No. 32, 444–449 (Sept. 1957).

Note on bounds for certain determinants. Emilie V. Haynsworth. Duke Math. J. **24,** No. 3, 313–320 (Sept. 1957).

Nonresonant absorption of symmetric top molecules. Shape of the nonresonant spectra. George Birnbaum. J. Chem. Phys. **27,** No. 2, 360–368 (Aug. 1957).

On the identity relationship for fractional replicates of the 2^n series. R. C. Burton and W. S. Connor. Ann. Math. Statistics **28,** No. 3 (Sept. 1957).

On the representation of a certain integral involving Bessel functions by hypergeometric series. Peter Henrici. J. Math. Physics **36,** No. 2, 151–156 (July 1957).

On the specification of transient nonequilibrium systems. Kurt E. Shuler. 6th Intern. Symposium on Combustion. 371–374 (1957).

Propagation of the radiofrequency ground wave transient over a finitely conducting plane earth. J. R. Johler. Geofis. pura e appl. **37,** 116–126 (May–Aug. 1957).

Shellac. C. C. Hartman. Offic. Dig. Federation Paint Varnish Production Clubs. **29,** No. 393, 1028 (Oct. 1957).

Scientists' and public's responsibility. Allen V. Astin. Phys. Today. **10,** No. 11, 23–27 (Nov. 1957).

Spectra of afterglows and discharges from nitrogen-oxygen mixtures. U. H. Kurzweg, A. M. Bass, and H. P. Broida. J. Mol. Spectroscopy. **1,** 184–200 (1957).

Hydrogen liquefaction by a dual pressure process. D. B. Chelton, J. Macinko, and J. Dean. Refrig. Eng. **65,** No. 8, 39–41 (Aug. 1957).

Bureau of Standards comments on Loran communications. E. K. Smith. IRE Trans. **ANE–4,** 84 (June 1957).

High-order harmonics for X-band oscillator stabilization. M. C. Thompson and J. V. Cateora. Rev. Sci. Inst. **28,** 656 (Aug. 1957).

Audio-frequency electromagnetic hiss recorded at Boulder in 1956, J. M. Watts. Geofis. pura e appl. **37,** 169–173 (May–Aug. 1957).

Conversion of payroll processes at the National Bureau of Standards from manual to punched cards. Paul R. McClennon. Federal Accountant. **7,** No. 2, 64–72 (Dec. 1957).

Characteristics and present requirements of ferrites. R. D. Harrington. Proc. Thirteenth Ann. Metal Powder Assoc. (1957).

Congruences for the coefficients of modular forms and some new congruences for the partition function. Morris Newman. Can. J. Research. **9,** (1957).

Mathematics.—A determinantal inequality of H. P. Robertson, I. Olga Taussky.—A determinantal inequality of H. P. Robertson, II. Marvin Marcus. J. Wash. Acad. Sci. **47,** No. 8, 263–266 (Aug. 1957).

Effect of illumination on the oxidation of copper single crystals in water. Jerome Kruger. J. Appl. Phys. **28,** No. 10, 1212–1213 (Oct. 1957).

Publications for which a price is indicated are available only from the Superintendent of Documents, U. S. Government Printing Office, Washington 25, D. C. (foreign postage, one-fourth additional). The three NBS periodicals are available on a 1-, 2-, or 3-year subscription basis. Reprints from outside journals and the NBS Journal of Research may often be obtained directly from the authors.

U. S. GOVERNMENT PRINTING OFFICE : 1958